

# Clinical Significance of Partial Volume Averaging of the Temporal Bone

Donald W. Chakeres<sup>1</sup>

The effects of partial volume averaging on computed tomographic images of temporal bone structures were evaluated. The models chosen for study included a cadaver stapes, two metallic prosthetic stapes, and a formalin-fixed temporal bone. The studies measured the changes in apparent dimension and Hounsfield units with incremental filling of voxels with metallic densities, changes in the angle of tomographic section in relation to small bony structures, and the effects of soft-tissue silhouetting. The clinical significance of these changes is demonstrated by examples of this phenomenon seen in actual patient examinations. This study confirms that partial volume averaging is one of the primary limitations in resolution of small structures of the temporal bone.

Partial volume averaging is a phenomenon that occurs with computed tomography (CT) when the dimensions of the object being imaged are smaller than the slice thickness and the individual voxel (the actual volume in space measured for a single pixel of the image) [1, 2]. Nonrepresentative Hounsfield units may be generated when all of the densities within an individual voxel are averaged to produce a single attenuation coefficient. Because many of the structures in the temporal bone are smaller than the standard voxel dimensions, this region is more susceptible to the effects of partial volume averaging than other areas of the body. In the temporal bone, structures with markedly different attenuation coefficients lie within the same voxel, such as when an ossicle of bone density is surrounded with air. The effects of partial volume averaging on temporal-bone imaging were studied using a series of model experiments on metallic prosthetic stapes, cadaver stapes, and formalin-fixed temporal bones. The results were compared with similar findings in actual patient examinations.

## Materials and Methods

### *Incremental Filling of Individual Voxels*

Two metallic wire prosthetic stapes were oriented within the CT gantry perpendicular to the tomographic section so that their long axes were parallel to the long axes of the individual voxels (fig. 1, positions 4 and 5). The Shea platinum stainless steel cup piston measured 5.0 mm in length and 0.6 mm in diameter (fig. 1, position 4). The House wire measured 4.75 mm in length and 0.005 mm in diameter with small loops at the ends of the prosthesis (fig. 1, position 5). The prostheses were sectioned at 1 mm increments. The initial sections contained only air, but with each succeeding section an increasing portion of the voxels was filled with the prosthetic stapes until the wire extended the full length of the voxel. The dimensions and Hounsfield units (measured with a range-of-interest cursor) for each of the CT images were recorded.

### *Effects of Change in Section Plane Angle*

To evaluate changes in the tomographic section angle on the partial volume averaging

Received May 25, 1983; accepted after revision November 22, 1983.

<sup>1</sup> Department of Radiology, Neuroradiology Section, University of Texas Health Science Center at San Antonio, and Audie Murphy Veterans Administration Hospital, 7703 Floyd Curl Dr., San Antonio, TX 78284.

**AJNR 5:297-302, May/June 1984**  
0195-6108/84/0503-0297 \$00.00  
© American Roentgen Ray Society

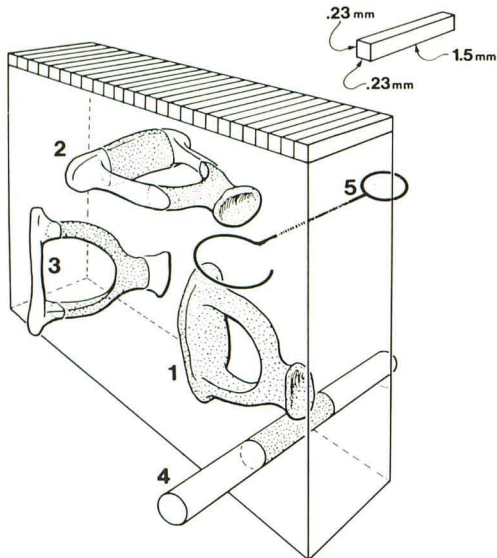


Fig. 1.—Dimensions and configuration of individual voxel used for CT of temporal bone are in upper right corner. Series of voxels defining line of pixels is at top of 3-D rectangle. Orientation of voxels to stapes in experimental positions 1, 2, and 3 and to two metallic prosthetic stapes (position 5 corresponds to House wire, and 4 corresponds to Shea piston) is shown. All models are depicted to scale to illustrate method by which they are sectioned.

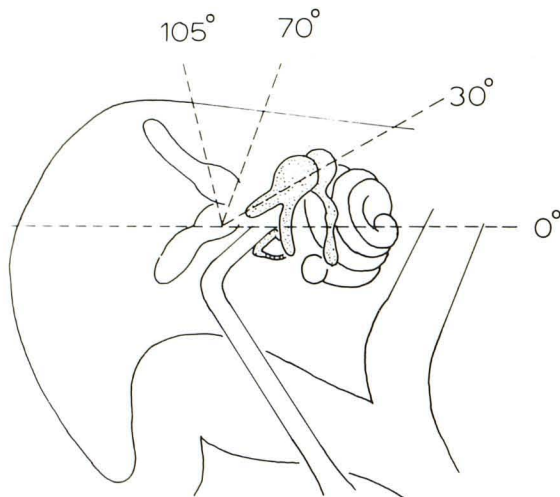


Fig. 2.—Lateral schematic diagram of temporal bone includes ossicles, cochlea, semicircular canals, facial nerve canal, jugular fossa, and carotid canal. Relation of anthropologic baseline ( $0^\circ$ ) to these structures is constant. The  $0^\circ$ ,  $30^\circ$ ,  $70^\circ$ ,  $105^\circ$  CT section planes have been found to allow for best overall evaluation of temporal bone. With the lateral scout view, these planes are easily identifiable. (Reprinted from [3].)

effects, a cadaver stapes was studied. The stapes was mounted (without a footplate) to the end of a toothpick with glue. This allowed for exact orientation of the stapes at selected angles within the CT scanner gantry. Two of the orientations were designed to correspond to normal coronal and axial tomographic sections of the stapes (fig. 1, positions 2 and 3). The third orientation with the plane containing the crus and neck of the stapes parallel to the tomographic section

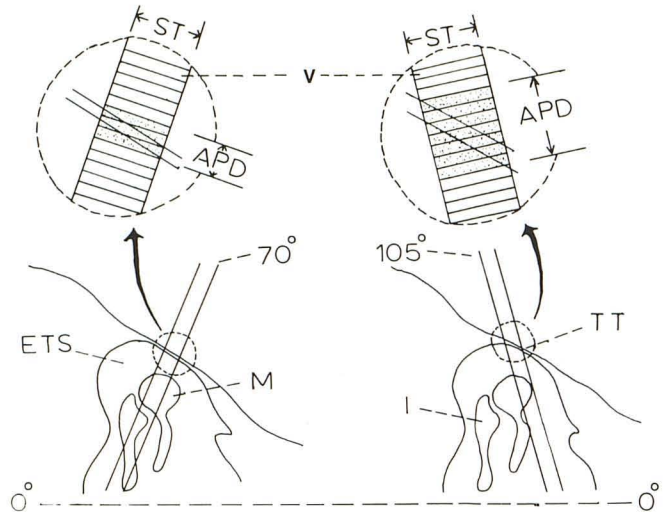


Fig. 3.—Orientation of individual voxels (V) to thin segment of tegmen tympani (TT). Structures are oriented to  $0^\circ$  anthropologic baseline. Lower diagram depicts malleus (M) and incus (I) in epitympanic space (ETS) as viewed in sagittal plane (lateral projection). Relation of CT section planes ( $70^\circ$ ,  $105^\circ$ ) to sloping tegmen tympani is shown. Blown-up detailed view of voxels with slice thickness (ST) dimension is demonstrated in relation to tegmen tympani on upper diagrams. Apparent pixel dimension (APD) is much greater for  $105^\circ$  section plane than for  $70^\circ$  plane, even though they are both imaging the same structure.

(and perpendicular to the voxels) was the ideal plane to study the stapes, but it is not possible to obtain this plane on patients (fig. 1, position 1).

The stapes was first oriented as it is imaged in routine coronal ( $105^\circ$  relative to the anthropologic baseline) tomographic CT sections (fig. 2) [3]. In this orientation the plane of the crus and neck of the stapes is parallel to the long axes of the voxels (fig. 1, position 2). Sections were made at 1 mm intervals. The same stapes was then rotated so that the plane containing the crus and neck of the stapes was perpendicular to the long axes of the voxels, and turned  $45^\circ$  from the tomographic section to simulate routine axial ( $30^\circ$ ) CT images (fig. 1, position 3). Finally, the same stapes was oriented with the plane of the neck and crus perpendicular to the long axes of the voxels, but aligned with the CT tomographic section (fig. 1, position 1). In this ideal presentation, the stapes was imaged as a Y-shaped density surrounded by air. The number of contiguous CT sections on which the stapes was visible, the dimensions, and the Hounsfield units were recorded for each orientation. The configuration and degree of resolution of the stapes were also noted.

To study the effect of changes of tomographic section plane on another small temporal bone structure, a formalin-fixed cadaver temporal bone was sectioned with a jeweler's saw in a sagittal plane through the medial external auditory canal. This exposed the tympanic tegmen to direct visualization. A segment of tegmen just lateral to the cochlea that measured less than 1 mm in thickness was chosen for study.

The temporal bone was first oriented in the CT scanner gantry so that the tomographic section was similar to the  $70^\circ$  section plane that is perpendicular to the tegmen (fig. 3). The segment of the tegmen chosen for study was then sectioned at 1 mm increments and the thickness was recorded. The temporal bone was then rotated to the  $105^\circ$  tomographic plane (similar to routine patient coronal CT images). In this orientation, the section plane is no longer perpendicular to the tegmen. The same segment of tegmen imaged earlier was

Fig. 4.—**A**, 1.5 mm section shows cadaver stapes (S) extending from toothpick (TP) when plane containing crura and body of stapes is perpendicular to tomographic section plane (fig. 1, position 2). This orientation is similar to routine coronal patient images. Stapes is seen as linear density with neck slightly denser near point of contact with toothpick. Metallic prosthetic House wire (HW) (fig. 1, position 5) is seen as small dot measuring -430 H, similar in density to adjacent toothpick. House wire was oriented so that it was perpendicular to tomographic section plane. The second metallic prosthetic stapes, a Shea piston (SP) (fig. 1, position 4) is seen as metallic density measuring 2000 H at right margin of toothpick. It has surrounding halo artifact. Because Shea piston totally fills voxel it is imaged as true metallic density. Segment of external auditory canal (EAC) of formalin-fixed temporal bone surrounds stapes to simulate middle ear cavity. **B**, 1 mm anterior. Shea piston does not appear metallic in density (75 H) because voxel was filled primarily with air. CB = cursor box measuring House wire.

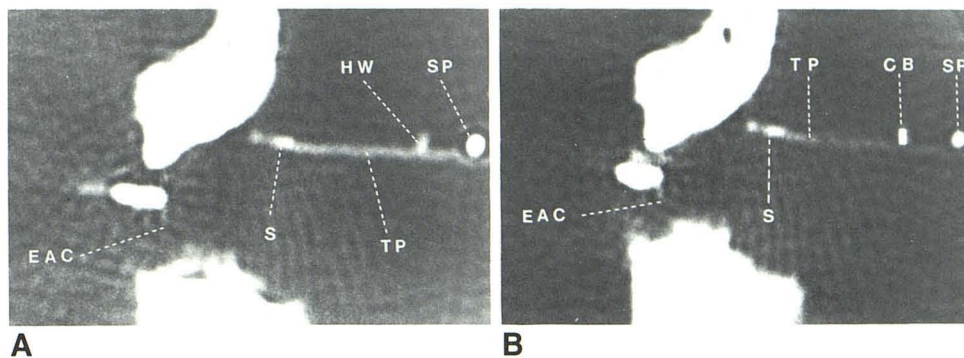
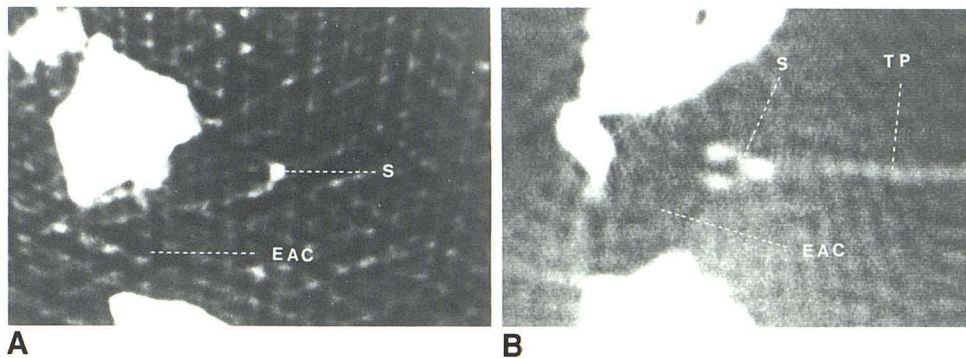


Fig. 5.—**A**, Neck of model stapes (S) is visible just lateral to segment of external auditory canal (EAC). On 1.5-mm-thick section stapes is oriented so that plane containing crura and body of stapes is perpendicular to voxels and rotated at 45° angle to tomographic section (fig. 1, position 3). Orientation is similar to routine axial patient CT sectioning. Because of partial volume averaging individual crura of stapes were only faintly identifiable. **B**, 1.5 mm CT section through cadaver stapes in fig. 1, position 1. Plane of crura and body of stapes parallels tomographic section, producing Y-shaped density. Remaining densities are related to formalin-fixed temporal bone, external auditory canal, and toothpick (TP) that surrounds model. Even though dimension of stapes is as small as 0.2 mm it is still resolved.



sectioned again, and the apparent thickness of the tegmen was recorded.

#### Soft-Tissue Silhouetting

To evaluate the effect of silhouetting by soft-tissue densities on partial volume averaging, the same cadaver stapes and toothpick used for the second study were embedded in a drop of wax. The plane of the neck and crus of the stapes was oriented perpendicular to the long axes of the voxels (fig. 1, position 1) and sectioned at 1 mm increments. The visibility, measurement of Hounsfield units, and dimensions of the stapes were recorded.

#### Patient Studies and Model Technique

The patients selected were referred for evaluation of primary abnormalities of the temporal bone, and examples were chosen because they demonstrated the effects of partial volume averaging. All of the CT studies were completed using a choice of four separate

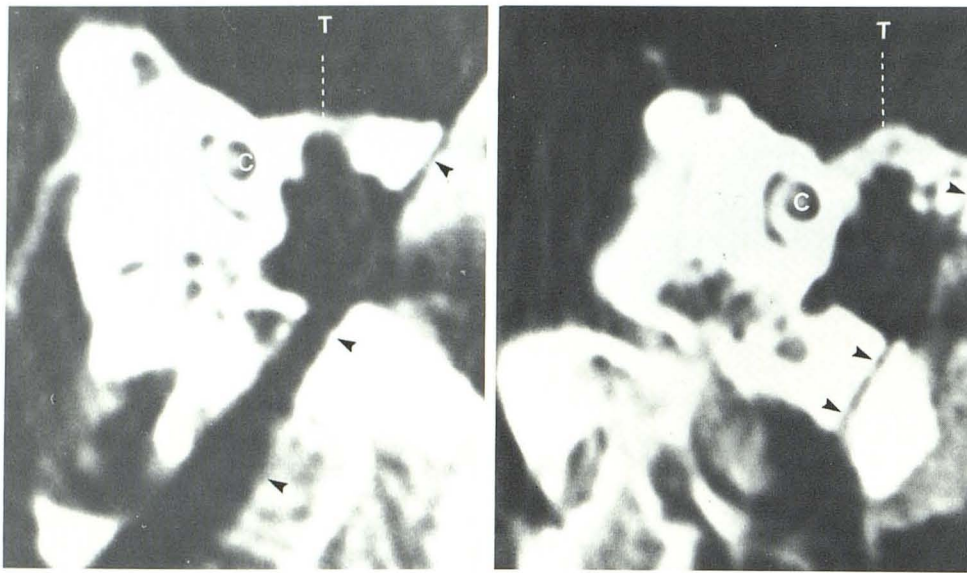
tomographic planes defined in relation to the anthropologic baseline (fig. 2) [3].

Using a General Electric 8800 CT/T body scanner, sections of 1.5 mm thickness were made using a 9.6 sec scan time, 576 views, bone algorithm program, targeted reconstruction (with a magnification factor of 3.5 or 4.0), and 200–384 mAs. The pixel dimensions measured 0.23 mm; therefore, the voxel volume measured  $0.23 \times 0.23 \times 1.5$  mm. All of the experimental studies were completed with water bags surrounding the models. A segment of formalin-fixed temporal bone, including the external auditory canal, was placed so that it surrounded the model stapes, simulating the normal middle ear cavity. All of the patient examinations were done with parameters similar to the model study.

## Results

#### Increment Filling of Individual Voxels

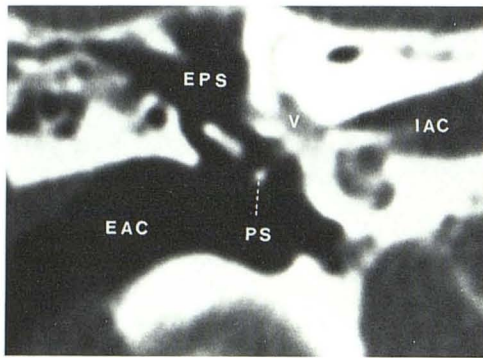
The measured Hounsfield units for the Shea prosthetic stapes ranged from 75 (fig. 4B), when only part of the voxel



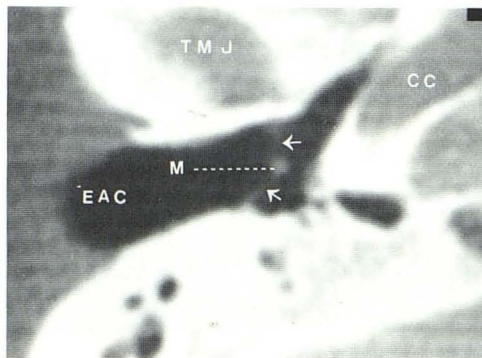
A

B

Fig. 6.—A, Segment of tegmen (T) in formalin-fixed temporal bone chosen for study is seen as thin, bony density when sectioned in 70° tomographic plane (fig. 3). Cochlea (C) is just medial to tegmen. Saw cut through external auditory canal exposing tegmen to direct visualization is labeled with *arrowheads*. B, After rotation to 105° tomographic plane (fig. 3). Same segment of tegmen just lateral to cochlea now appears to be thicker because it is oriented obliquely to tomographic section. *Arrowheads* mark saw cut made through temporal bone.



7



8

Fig. 7.—5-mm-thick CT section through external auditory canal in 105° tomographic plane in patient with prosthetic stapes (Robinson wire). Tip of metallic prosthetic stapes (PS) has nonmetallic density on section since only part of it fills individual voxel. Prosthesis on more posterior sections was clearly metallic in density. EAC = external auditory canal; EPS = epitympanic space; V = vestibule; IAC = internal auditory canal.

Fig. 8.—1.5 mm CT image at 30° tomographic plane through external auditory canal (EAC). Part of temporomandibular joint (TMJ) and carotid canal (CC) are visible. Tympanic membrane (*arrows*) is visible as linear density on 30° axial tomographic plane because it is thickened. Suspended umbo of malleus (M) is present centrally. This patient had a long history of chronic inflammatory changes with thickened tympanic membrane documented at surgery. Opposite normal tympanic membrane was not visible.

was filled, to 2200 (the expected measurement for metallic density) (fig. 4A), when the stapes filled the voxel. This large prosthesis was easily visible and was surrounded by a circular scan artifact. The House wire prosthetic stapes was visible as a low-density dot measuring  $-430$  H (fig. 4A).

#### Varying Section Plane Angle

When sectioned in a fashion similar to coronal CT imaging (fig. 1, position 2), the mounted stapes was visualized as a linear density extending from the toothpick (fig. 4). The neck of the stapes was denser than the crus, but did not appear to be of bony density. The stapes measured about  $-460$  H and was seen on five contiguous 1 mm incremental images.

When the stapes was oriented similar to axial imaging (fig.

1, position 3), both crura of the stapes were poorly visualized. The neck of the stapes measured about  $-500$  H and was identifiable (fig. 5A).

Finally, the stapes was imaged as a Y-shaped structure (fig. 5B) when the plane of the crus and neck were oriented perpendicular to the voxels (fig. 1, position 1). It measured  $-500$  H and was visualized on two contiguous 1 mm incremental sections.

The section of tegmen chosen for study in the formalin-fixed temporal bone when sectioned in the 70° tomographic plane (fig. 3) measured less than 2 mm in thickness (fig. 6A). When the same temporal bone was rotated to the 105° coronal tomographic section plane with the tegmen oblique to the section plane (fig. 3) the selected section of tegmen measured 5 mm in thickness (fig. 6B).

### *Soft-Tissue Silhouetting*

The stapes was barely perceptible when embedded in wax and sectioned in an identical fashion as the same stapes in the earlier study (fig. 1, stapes position 1). The stapes produced only a faint Y density within the wax and measured -220 H.

### *Clinical Examinations*

The most common implication of the phenomenon of partial volume averaging on our actual patient studies was the nonvisualization of small structures such as the tympanic membrane, the stapes, the long process of the incus, the individual septa of the mastoid air cells, the tegmen, the margins of the facial nerve canal, and the vestibular aqueduct. Small, dense structures such as the ossicles were found to measure well below the expected Hounsfield units for bone when surrounded by air. Soft-tissue densities may silhouette small dense structures if they are contiguous. Many small components of the temporal bone were found to extend beyond their known anatomic location by a distance of less than the slice thickness.

### **Discussion**

Partial volume averaging was recognized early in the development of CT as a significant limitation and artifact [4, 5] of this method. Some investigators believed that partial volume averaging was not a significant problem and assumed that substitution of known attenuation coefficients for structures being averaged within an individual voxel would allow for accurate prediction of Hounsfield units [6]. This hypothesis was proven incorrect by more extensive investigation, which showed that the spatial orientation of structures within the CT scanner gantry in the individual voxels significantly influenced the measured Hounsfield units in a nonlinear and unpredictable manner [7, 8].

Our study more closely approximates the true clinical setting than prior studies, in which the specific phantoms were dissimilar to anatomic structures in their configuration and density. This study explains many of the commonly seen imaging aberrations of the temporal bone and other small bony structures (lamina papyracea, cribriform plate, septations within the ethmoid air cells and floor of the sella) in the routine clinical setting.

### *Incremental Filling of Voxels*

Erroneously low Hounsfield-unit measurements for small, dense structures are explained by this study. A clinical example of this is the low Hounsfield-unit measurements obtained for large metallic prosthetic stapes when sectioned at their extremes (fig. 7). Since the House wire is so fine, it is not visible on CT images of patients, even though it is metallic. Also, the same dense structure may appear to extend beyond its known anatomic location by less than the slice thickness. For example, the stapes (fig. 1, position 1) was seen on two

contiguous sections, suggesting that it was 2 mm in thickness, when its actual measurement was only 0.4 mm. The prostheses may also appear to extend slightly beyond their expected location both anteriorly and posteriorly on coronal sections.

### *Effects of Change in Section Plane Angle*

The tympanic membrane (fig. 8) and stapes are seen frequently on coronal CT images, but rarely on axial images, because the voxels in the coronal tomographic plane are oriented so that they are filled to a greater degree by these individual structures. A similar phenomenon is seen with the varying appearance of the lung fissures by CT [9]. There are other causes that account for nonvisualization, including patient motion, computer algorithm, and the inherent spatial resolution limits of CT. Spatial resolution is a function of many complex variables, with partial volume averaging only one of them. Occasionally, the tegmen and other thin, bony margins may not be visible. This nonvisualization can be related to partial volume averaging rather than a true abnormality. Thin, dense, bony septa may appear thicker than their true dimensions when oriented obliquely through a series of adjacent voxels (fig. 6).

### *Soft-Tissue Silhouetting*

Silhouetting of small, dense structures may occur when soft-tissue densities, such as normal adjacent brain, hemorrhage, tumor, or fluid (fig. 9) envelop or are contiguous with a structure usually bordered by air. Even though the actual Hounsfield units for these small structures are larger when silhouetted than when surrounded by air, the difference in density between the structures and the background density may be insufficient for their visualization. This is important in the evaluation of ossicular abnormalities in conjunction with soft-tissue masses or small erosions (fig. 9).

A similar imaging aberration occurs when small canals, such as the vestibular and cochlear aqueducts, or lucencies, such as fractures, are not visualized. Since most of the voxels in these cases are filled with dense bone, the lucency is lost (fig. 10).

### *CT Limitations*

Partial volume averaging is a major limitation in the evaluation of the temporal bone by CT. Increasing the radiation dose will not resolve the problem. Although an increased radiation dose helps to differentiate low-contrast objects, the temporal bone is an inherently high-contrast subject [10, 11]. The low Hounsfield-unit measurement of small, dense structures will persist no matter how much radiation is used, because it is a result of partial volume averaging rather than true low density. Thinner CT slice thickness would be the only means of overcoming this phenomenon, but submillimeter slice thickness would require a higher x-ray tube output and many more sections per examination. It is possible that these parameters will be available in the future.

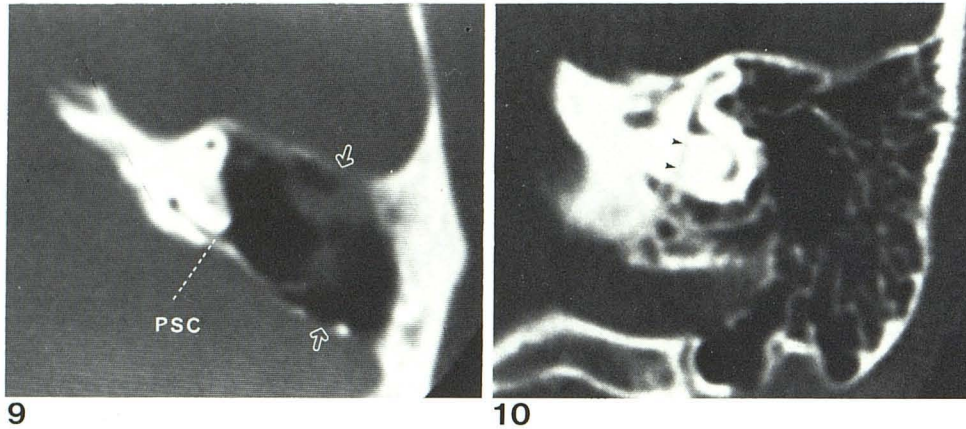


Fig. 9.—1.5-mm-thick CT section of left temporal bone at 30° tomographic section plane through superior and posterior semicircular canals. Erosion involving posterior semicircular canal (PSC) secondary to large destructive cholesteatoma filling mastoid air cells. Anteriorly and posteriorly, there appear to be multiple erosions of temporal bone with dura in direct contact with cholesteatoma cavity (arrows). At surgery, no exposed dura was seen. This finding is secondary to silhouetting of margins by adjacent soft-tissue densities and partial volume averaging.

Fig. 10.—Complete vestibular aqueduct (arrowheads) is seen extending inferiorly from region of common crus of posterior and superior semicircular canals. This 70° tomographic section parallels course of vestibular aqueduct, which allows for its visualization. In most cases this small bony canal is masked on coronal sectioning by effects of partial volume averaging.

Even though CT has excellent contrast and spatial resolution, inherent physical problems of partial volume averaging will limit its accuracy. Since no computer software solution is available to solve this scanning artifact, recognition is the most important clinical solution. Orienting the temporal bone structures to specific section planes will diminish or enhance the partial volume effect. Therefore, two section planes, one axial and one coronal, should be used to produce the maximum amount of information and limit the errors in diagnosis.

#### ACKNOWLEDGMENTS

I thank Linda Chakeres and Beverly Combs for editorial and secretarial assistance.

#### REFERENCES

- Zatz L. General theory of computed tomography. In: Newton TH, Potts DG, eds. *Radiology of the skull*, vol 5. *Technical aspects of computed tomography*. St. Louis: Mosby, 1981:3853-3876
- Pullan BR, Ritchings RT, Isherwood I. Technical aspects of computed tomography. In: Newton TH, Potts DG, eds. *Radiology of the skull*, vol 5. *Technical aspects of computed tomography*. St. Louis: Mosby, 1981:3911-3912
- Chakeres DW, Spiegel PK. A systematic technique for comprehensive evaluation of the temporal bone by computed tomography. *Radiology* 1983;146:97-107
- Joseph PM. Artifacts in computed tomography. In: Newton TH, Potts DG, eds. *Radiology of the skull*, vol 5. *Technical aspects of computed tomography*. St. Louis: Mosby, 1981:3985-3987
- Goodenough DJ, Weaver KE, Davis DO. Potential artifacts associated with scanning patterns of the EMI scanner. *Radiology* 1975;117:615-619
- Turner H, Houdek PV, Trefler M. Measurements of the partial volume phenomenon. *Comput Radiol* 1979;3:213-219
- Goodenough D, Weaver K, Davis D, LaFalce S. Volume averaging limitations of computed tomography. *AJR* 1982;138:313-316
- Glover GH, Pelc NJ. Nonlinear partial volume artifacts in x-ray computed tomography. *Med Phys* 1980;7:238-248
- Marks BW, Kuhns LR. Identification of the pleural fissures with computed tomography. *Radiology* 1982;143:139-141
- Blumenfeld SM, Glover G. Spatial resolution in computed tomography. In: Newton TH, Potts DG, eds. *Radiology of the skull*, vol 5. *Technical aspects of computed tomography*. St. Louis: Mosby, 1981:3918-3940
- Bergstrom M. Performance evaluation of scanners. In: Newton TH, Potts DG, eds. *Radiology of the skull*, vol 5. *Technical aspects of computed tomography*. St. Louis: Mosby, 1981:4221-4222